IEEE Access
Multidisciplinary | Rapid Review | Open Access Journal

Received February 25, 2018, accepted April 17, 2018, date of publication April 27, 2018, date of current version May 16, 2018.

Digital Object Identifier 10.1109/ACCESS.2018.2829723

Adaptive Control and Predictive Control for Torsional Vibration Suppression in Helicopter/Engine System

YONG WANG[1], QIANGANG ZHENG[1], HAIBO ZHANG[1], AND LIZHEN MIAO[2]

[1]Jiangsu Province Key Laboratory of Aerospace Power Systems, College of Energy and Power Engineering, Nanjing University of Aeronautics and Astronautics, Nanjing 210000, China
[2]China Gas Turbine Establishment, Chengdu 610000, China

Corresponding author: Haibo Zhang (zh_zhhb@126.com)

This work was supported in part by the National Natural Science Foundation of China under Grant 51576096, in part by the Qing Lan 333 Project and Foundation of Graduate Innovation Centre in NUAA under Grant kfjj20170221, and in part by the Fundamental Research Funds for the Central Universities.

ABSTRACT In order to damp torsional vibrations in a helicopter, which would cause resonance in rotating components like engine, transmission, and rotor, an adaptive notch filter is proposed. Instead of fixed notch filter, the adaptive one, with FFT analyzer and sorting algorithm, can damp the low-order torsional vibration signal with natural frequency varying in a wide range. Then, in order to enhance the power following capability of the engine, a nonlinear model predictive controller based on the supported vector machine is designed to compensate for the dynamic control performance. Through the adaptive notch filter, the torsional vibration of the free turbine speed whose frequency is away from the set-point value can effectively be suppressed by 50% compared with the fixed notch filter. Furthermore, instead of conventional PID controller, the nonlinear model predictive controller based on the adaptive notch filter can reduce the sag of the free turbine to less than 0.4%. Therefore, the control strategy achieves fast high-quality response of the turbo-shaft engine.

INDEX TERMS Helicopter, torsional vibration, adaptive control, predictive control.

I. INTRODUCTION

Helicopter is a multiple-degree-of-freedom and strong- coupling system with precise and complex design process and control system. There is only one load channel from the engine to the rotor, and any failure of any part of the channel will pose a serious threat to flight safety [1]. Therefore, in the aspect of structure and power, the torque drive chain of helicopter is irredundant and critical [2].

One of the design principles of the turbo-shaft engine is to ensure that the engine output speed is constant, does not pulsate and does not deviate from the steady-state value in steady-state flight. If the engine output speed pulsates, the speed sensor can feel the variation, and the fuel flow will change through the fuel adjustment system to correct the speed. Therefore, if the output shaft speed pulsates, the fuel flow will pulsate accordingly. The two systems form a closed-loop coupling and self-excited vibration system. Under certain conditions, the difference of the phase between the fuel flow and the output speed is the power to the vibration system. If the input energy exceeds the damping of the system (such as the damping of the rotor damper, etc.), the unstable self-excited vibration will occur [3]. Thus, the torsional vibration is an unavoidable and basic problem in the design of helicopter/engine control system.

Research on torsional vibration modeling and control of helicopter/engine coupling system was carried out early abroad. Boeing and Sikorsky discovered torsional problems in the 1960s and 1970s [4]–[6]. In the 1970s and 1980s, the dynamics and modeling techniques of the engine were studied abroad [7], [8], and a number of solutions have also been introduced, where vibration dampers were utilized early, and replaced by notch filters later [9]–[11]. The analysis and processing of the dynamics of the S-76 helicopter is very successful [12]. In the control scheme, in 1998, Hansford and Vorwald [13] proposed and used the impedance matching method to analyze the torsional vibration problem of helicopter. In the study of the rotor speed control, to suppress the torsional vibration signal in the feedback loop,

the series notch filter in the speed closed-loop of free turbine is used [14]–[17]. Due to rather large additional phase shift in the low-frequency stage, Quan *et al.* [18] proposed multiple notch filters in parallel. Thus, according to the different working conditions of the engine, different filters will be chosen. The method can not only suppress the torsional vibration signal well, but also reduce the influence of additional phase introduced into the system.

In order to simplify the design process of the torsional vibration suppression and avoid the deterioration of operating efficiency of the turbo-shaft engine, the fixed rotor speed control is used in the conventional rotorcrafts. That is, the transmission ratio of the power transmission chain is constant. In this case, the torsional vibration frequency is fixed, thus the fixed notch filter is widely applied in the speed closed-loop control of modern turbo-shaft engine. In the variable rotor speed case, however, the frequency and amplitude of the torsional vibration signal vary with the rotor speed. Instead of fixed one, the adaptive notch filter with good following performance [19], [20] can better damp the coupling torsional vibration and achieve high control effect quality. There have been many adaptive torsional vibration absorbers available in recent years, but many of them may cause time delay and too much computing time.

During the process of variable rotor speed, the helicopter demanded torque and the engine output torque match each other through the variable ratio clutch that enhances the coupling between the helicopter subsystem and the engine subsystem. Thus, in terms of the traditional cascade PID with total moment feed-forward, it is very difficult to obtain high quality control effect [21], [22]. Especially in the maneuvering flight, there is a non-negligible delay caused by the rotor torque measurement and the engine dynamic control response. In the minor time scale of maneuvering flight, this delay must be considered in the design of control law. The cascaded PID does not have the prediction function, and it will not have good performance in this situation mentioned above. The model predictive controller [23], [24] has the tolerance to the model (parametric or nonparametric, linear or non-linear), the validity of finite time-domain rolling optimization and the possibility of considering various soft and hard constraints, if applied to the engine control system, it will be no doubt a desired control program. The predictive scheme can refer to the study of turbofan engine control system [25]–[29].

Therefore, In terms of the lack of researches on torsional vibration suppression in helicopter/engine system, the research proposes and designs an adaptive notch filter (ANF) by using the FFT, search algorithm and the fixed notch filter, based on UH-60 model combined with the simplified helicopter torsional vibration model. In order to further enhance the power following capability of the engine, reduce the sag and overshoot of the free turbine speed, the nonlinear model predictive controller (NMPC) is designed. In this case, the helicopter demanded torque prediction model and the turbo-shaft engine state parameter model established by supported vector machine (SVM) and the feasible sequence quadratic programming (FSQP) algorithm are utilized together to realize the fast response control of the turbo-shaft engine.

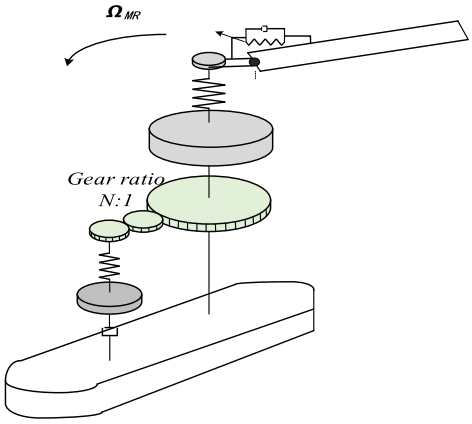

FIGURE 1. Model diagram of torsional vibration system.

II. HELICOPTER/ENGINE TORSIONAL VIBRATION MODEL

In the power transmission process of helicopter, through the reducer and drive shaft, the free turbine of the turbo-shaft engine drives the rotor and the tail rotor. All these high-speed rotating transmission parts together form a torque transmission chain of helicopter.

In order to truly reflect the dynamic behavior of the whole system as much as possible, and take active control to the helicopter torsional vibration, a simplified helicopter torsional vibration model needs to be established. The model is based on several assumptions: in the torque transmission chain, apart from the rotor and tail rotor, other rotation structures can be simplified as two-node torsion unit and centralized mass unit. Meanwhile, the power of the tail rotor is so small that the torque can be ignored. In addition, the structural distortion, the elastic deformation of the rotor, the helicopter body and the pneumatic damping can be neglected. According to these assumptions, the helicopter torsional vibration system is a damping torsional vibration system with five degrees of freedom and the structure as shown in Fig. 1, which consists of the collective lead-lag rotation of the blades, the hub, the transmission output, the rotating part of the engine, and the fuselage. The blades are connected to the hub through an offset hinge, spring and damper. The hub is connected to the transmission output through a shaft spring. The transmission output is free to rotate in the fuselage but connected to the engine through a reduction gear and a spring. The engine is free to rotate in the fuselage through a damper.

The torsional vibration equation is shown below, which is a basic second-order ordinary differential equation with five degrees of freedom.

$$\boldsymbol{M}\ddot{\psi} + \boldsymbol{C}\dot{\psi} + \boldsymbol{K}\psi = \boldsymbol{F} \tag{1}$$

where $\boldsymbol{M}$, $\boldsymbol{C}$, $\boldsymbol{K}$, $\boldsymbol{F}$ represent the matrix of inertia, damping, stiffness and force, and N is the gear ratio.

The rotational displacement of ψ vector is:

$$\begin{bmatrix} \psi_F \\ \psi_E \\ \psi_T \\ \psi_H \\ \psi_B \end{bmatrix} = \begin{bmatrix} \psi_{FI} \\ \psi_{EI}/N - \boldsymbol{\Omega}_{MR}t \\ \psi_{TI} - \boldsymbol{\Omega}_{MR}t \\ \psi_{HI} - \boldsymbol{\Omega}_{MR}t \\ \psi_{BI} - \boldsymbol{\Omega}_{MR}t \end{bmatrix} \tag{2}$$

where, ψ_F, ψ_T, ψ_H, ψ_B represent the torsional vibration displacements of fuselage, transmission, hub and blade separately, which equal to the component that the absolute displacements ψ_{FI}, ψ_{TI}, ψ_{HI}, ψ_{BI} minus the displacements caused by rotor speed $\boldsymbol{\Omega}_{MR}$.

The engine absolute displacement ψ_{EI} is different. Because of the gear ratio, a unit displacement of the transmission is in some sense equivalent to N units of engine displacement.

Supposing that the solution of Eq. (1) is the form as $\psi = Ce^{st}$, where $s = \sigma + i\omega$ is plural, σ is the damping, ω is the natural vibration angular frequency, C is a constant. Therefore, the natural vibration equation of Eq. (1) can be expressed as follows.

$$(\boldsymbol{M}s^2 + \boldsymbol{C}s + \boldsymbol{K})\psi = \boldsymbol{0} \tag{3}$$

To make ψ a non-zero solution, the sufficient condition is:

$$\det(\boldsymbol{M}s^2 + \boldsymbol{C}s + \boldsymbol{K}) = \boldsymbol{0} \tag{4}$$

Taking the UH60 helicopter/T700 engine at the rotor speed $\boldsymbol{\Omega}_{MR}$ of 30 rad/s as a research example, the ten solutions of Eq. (4) are obtained as follows.

$$\begin{aligned} s = & \ 0 \\ & 0 \\ & 0 \\ & -0.2857 \\ & -22.1356 \\ & -507.5016 \\ & -2.3911 \pm 12.3002i \\ & -0.6173 \pm 329.5269i \end{aligned}$$

That is, the natural vibration frequency of each order is:
0 order: 0rad/s = 0Hz
1st order: 12.3002rad/s = 1.9576Hz
2nd order: 329.5269rad/s = 52.4458Hz

Torsional vibration natural frequency consists of low order and high order. Both of them locate in different range, thus, different suppression scheme can be used. The high-order one is 52.25Hz, which can be filtered by the low-pass filter. However, the low-order one is close to 0Hz, instead of low-pass filter, a notch filter can be adopted, which can filter out a specific frequency.

When $\boldsymbol{\Omega}_{MR}$ increases from 0rad/s to 135rad/s. the variation of low-order natural vibration frequency is shown in Fig. 2.

Fig.2 summarizes the low-order natural vibration frequency under different rotor speed. As shown in Fig. 2, the natural vibration frequency varies in a broad range with the change of $\boldsymbol{\Omega}_{MR}$. Unfortunately, in this case, the notch filter with constant coefficient is hardly applicable. On the contrary, the notch filter with adaptive ability is badly in need.

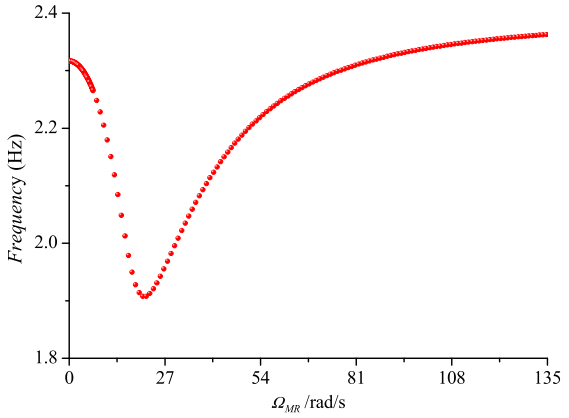

FIGURE 2. Low-order natural vibration frequency under different rotor speed.

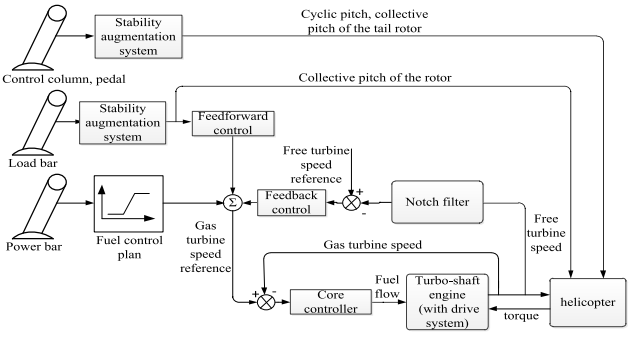

FIGURE 3. Conventional control structure of the turbo-shaft helicopter/ engine.

III. ADAPTIVE CONTROL

In order to avoid the torsional vibration of the free turbine, the direct method is to make compensation at the free turbine to change the amplitude and frequency curve of the open loop. The torsional vibration filter in the control system of turbo-shaft engine is shown as Fig. 3.

The design of the notch filter is based on the simplified helicopter torsional vibration model described above. The open-loop transfer function of the model is.

$$\frac{b_0 s(b_1 s + a_1)(c_2 s^2 + b_2 s + a_2)}{s^3(s + d_1)(s + d_2)(s + d_3)(s^2 + e_4 s + d_4)(s^2 + e_5 s + d_5)} \tag{5}$$

Quadratic polynomials in the denominator $s^2 + es + d$ is a second-order torsional vibration block, which can be written as $s^2 + 2\zeta_n\omega_n s + \omega_n^2$. ω_n represents the natural angular frequency of the torsional vibration model. As mentioned above, instead of the high-order torsional vibration, only considering the low-order one is enough. Increasing the damping coefficient ζ_n to ζ_N is able to suppress the torsional vibration,

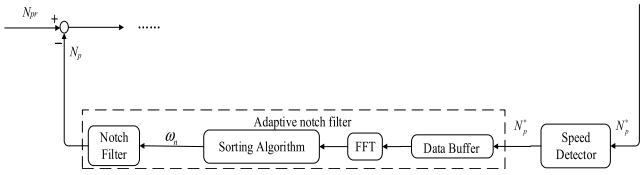

FIGURE 4. Block diagram of the adaptive notch filter in the feedback loop.

and the notch filter can be expressed as follows.

$$G(s) = \frac{s^2 + 2\zeta_n \omega_n s + \omega_n^2}{s^2 + 2\zeta_N \omega_n s + \omega_n^2} \tag{6}$$

When the notch filter is applied, the second order oscillation link in the system will be as follows.

$$\frac{\omega_n^2}{s^2 + 2\zeta_N \omega_n s + \omega_n^2} \tag{7}$$

The peak value at the oscillating frequency will be effectively reduced.

However, when the torsional vibration signal changes, that is, when the ω_n and ζ_n change, because the ω_n, ζ_n in Eq. (6) is fixed, only the torsional vibration frequency at set-point value can be filtered out. In this case, the notch filter cannot achieve the best performance. Under this circumstance, the ANF may be used. Based on the recursive algorithm, it can complete the filtering operation in the case of unknown amplitude-frequency information of torsional vibration. It means off-line calculation of the model is not necessary. It can track the change of the statistical characteristic of the torsional vibration signal with time. In the frequency domain analysis of the time domain signal, the fast Fourier transform (FFT) has a good performance. Therefore, when the torsional vibration signal changes, the variable ω_n could be distinguished by the FFT. The block diagram of the adaptive notch filter is shown below.

Fig. 4 shows the block diagram of the ANF. Firstly, the relative speed data N_p* is stored in a short time, which is performed by the speed detector and the data buffer. Then, the FFT method analyzes the stored digital speed in real time. The FFT can well and easily transform data from time domain to frequency domain to obtain the vibration information. Here, rather than the globe data, a windowed data is utilized as the input data of the FFT analyzer to get the real-time information of the signal. Thirdly, with a sorting algorithm, the dominant frequency of the maximum magnitude of the signal in frequency domain can be sorted out. Based on the dominant frequency of the maximum magnitude, the coefficients of the digital notch filter can be determined. Finally, with this ANF, the relative speed of free turbine N_p without torsional vibration interference is outputted.

The simulation of UH-60 model combined with the simplified helicopter torsional vibration model under variable rotor speed has been conducted at flight altitude $H = 500m$ and flight speed $V_x = 10m/s$. Fig. 5. (a)-(h) summarize N_p and the amplitude-frequency curve of N_p through FFT before and after ANF under different rotor speed. The sampling frequency is 50Hz, and in order to observe the low-order torsional vibration frequency, a step perturbation with amplitude 30% of rotor demanded torque is applied during 9-10s and the component of previous 15Hz is only drawn in the figure. As shown in the figure, when the rotor speed is close to 30rad/s, the torsional vibration frequency is approximately equal to 1.96Hz. In this case, the filtering effect of the fixed notch filter and ANF is similar. However, while the rotor speed is away from 30rad/s, the ANF can reduce the low-order torsional vibration signal by 50% compared with the fixed notch filter. Fig. 5. (j)-(l) show $\mathbf{\Omega}_{MR}$, N_p and the amplitude-frequency curve of N_p through FFT under continuously variable rotor speed. When the variable speed instruction is applied (as shown in Fig. 5. (i)), the $\mathbf{\Omega}_{MR}$ changes continuously along the specified path, where the low-order vibration frequency varies from 1.25Hz to 2.35Hz. In this case, the fixed notch filter can effectively suppress the torsional vibration at set-point value, but it is of little use to other frequencies beyond its bandwidth. Nevertheless, the ANF can still damp all torsional vibration signals remarkably with the amplitudes decreased by over 70% compared with those without any filters.

IV. PREDICTIVE CONTROL

In the case of variable rotor speed, the change of surge margin is more irregular due to the variation of free turbine flow capacity and efficiency. At the same time, the conventional control strategy is simple and easy, but the ability to follow the demanded power is poor. In order to optimize the helicopter energy efficiency and obtain better performance, high-quality response control of turbo-shaft engine is achieved by increasing the power following capability of the engine and reducing the amount of sag and overshoot of the free turbine speed.

The control block diagram is shown in Fig. 6. The ANF is added in the engine output speed loop, and together with the helicopter model constitutes the control object. The NMPC includes three parts: the helicopter demanded torque model, the turbo-shaft engine state parameter model and the rolling iterative algorithm.

The helicopter demanded torque model and the turbo-shaft engine state parameter model are both established based on supported vector machine. Through the past and the current input and flight status, the helicopter demanded torque model could predict the trend of the future torque. Thus, it can reduce the dynamic changes in the demanded torque and the engine output torque, thereby further reducing the dynamic interference and the torsional vibration. The torque estimation model is expressed as follows and the subscript indicates the time. N_1, N_2, N_3, N_4, N_5, N_6, N_7, N_8 are set to 2 [30], and the specific meaning of the parameter is shown in the symbol table. Then helicopter demanded torque model can be expressed as:

$$\boldsymbol{Y}_H = Q_H(k) = Pm_H(\boldsymbol{X}_H) \tag{8}$$

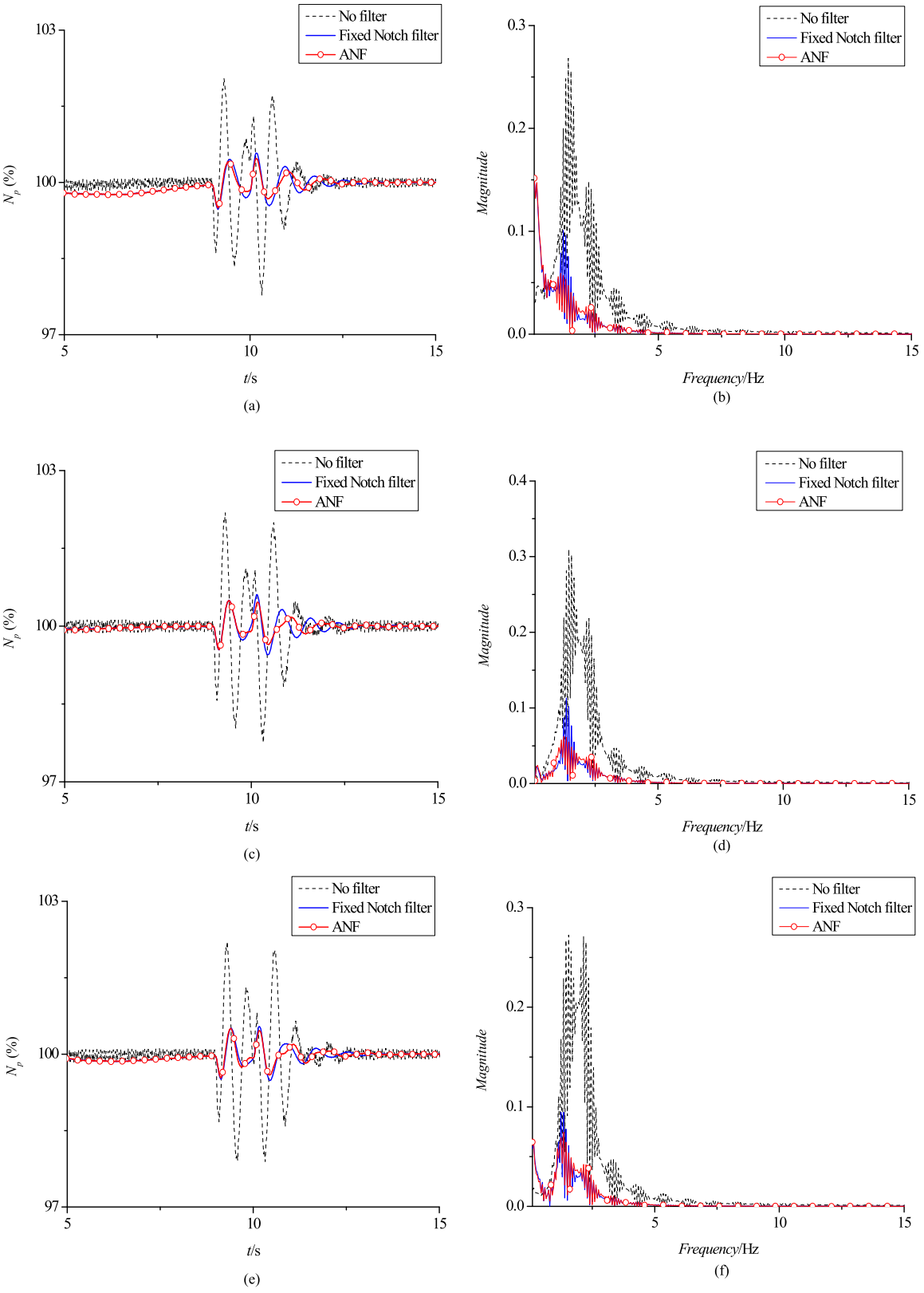

FIGURE 5. Torsional vibration simulation of ANF under different rotor speed. (a) N_p at $\Omega_{MR} = 22$rad/s. (b) FFT of N_p at $\Omega_{MR} = 22$rad/s. (c) N_p at $\Omega_{MR} = 27$rad/s. (d) FFT of N_p at $\Omega_{MR} = 27$rad/s. (e) N_p at $\Omega_{MR} = 33$rad/s. (f) FFT of N_p at $\Omega_{MR} = 33$rad/s.

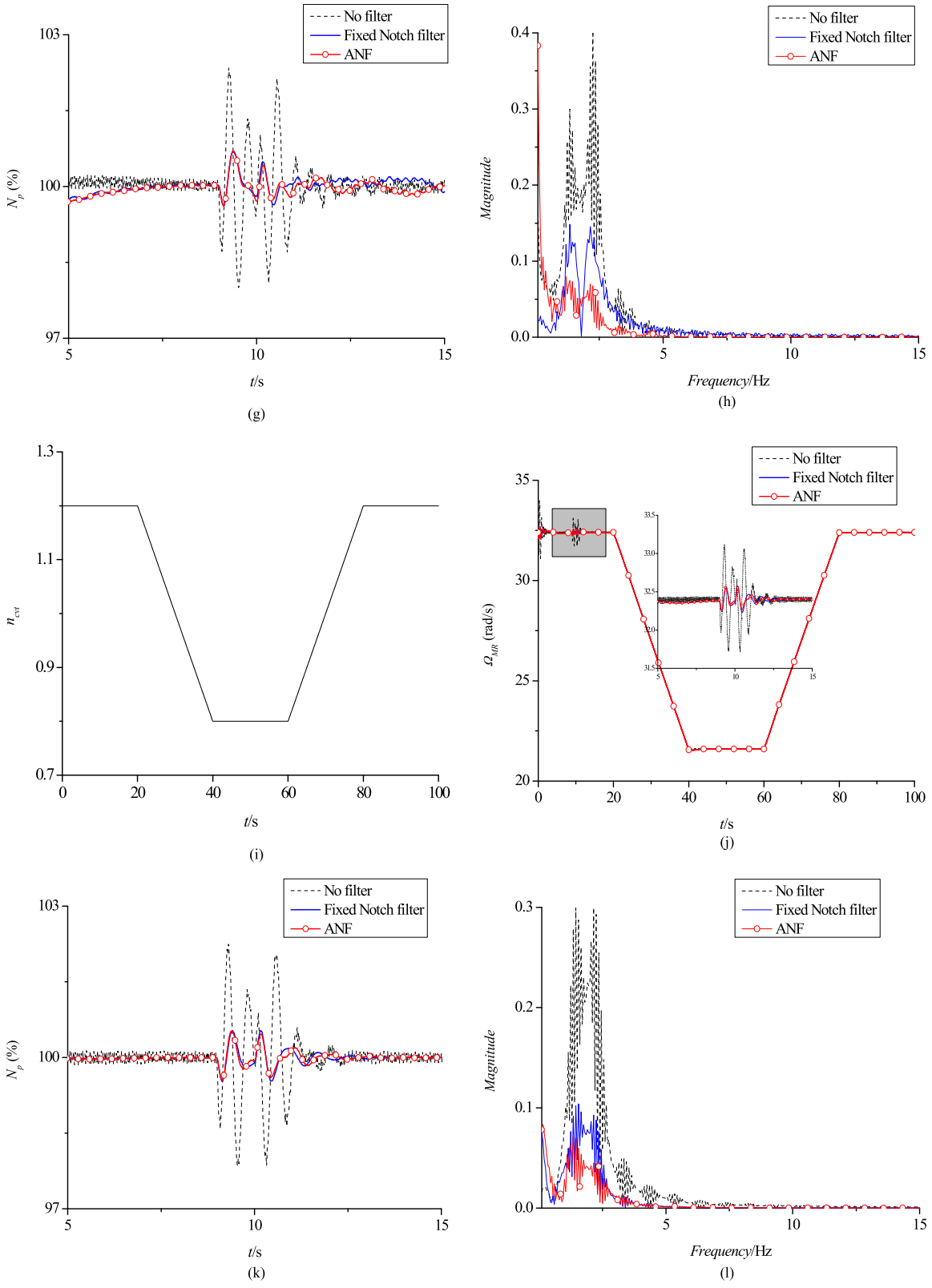

FIGURE 5. ***Continued.*** **Torsional vibration simulation of ANF under different rotor speed. (g) N_p at Ω_{MR} = 41rad/s (h) FFT of N_p at Ω_{MR} = 41rad/s. (i) Variable speed instruction. (j) Rotor speed Ω_{MR}. (k) N_p under continuously variable rotor speed. (l) FFT of N_p under variable rotor speed.**

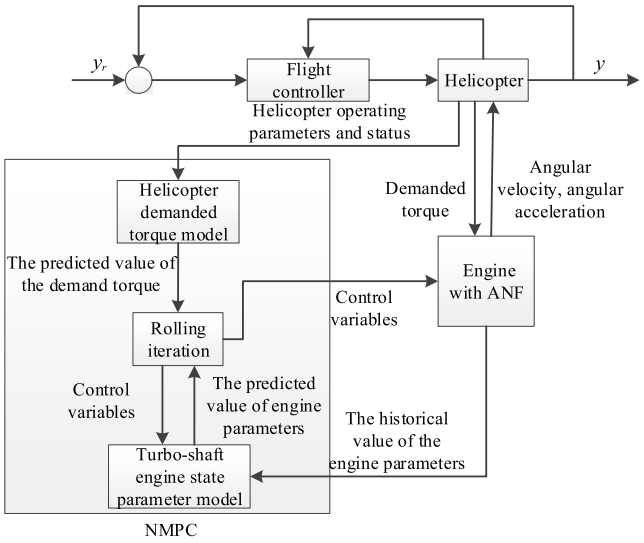

FIGURE 6. Helicopter integrated control block diagram.

where

$$\begin{cases} \boldsymbol{X}_H = [H_{(k)}, H_{(k-1)}, \ldots, H_{(k-N_1)}, V_{x(k)}, \\ \quad V_{x(k-1)}, \ldots, V_{x(k-N_2)}, \\ \quad V_{z(k)}, V_{z(k-1)}, \ldots, V_{z(k-N_3)}, \theta_{(k)}, \theta_{(k-1)}, \ldots, \theta_{(k-N_4)}, \\ \quad B_{1S(k)}, B_{1S(k-1)}, \ldots, B_{1S(k-N_5)}, A_{1C(k)}, \\ \quad A_{1C(k-1)}, \ldots, A_{1C(k-N_6)}, \\ \quad \boldsymbol{\Omega}_{MR(k)}, \boldsymbol{\Omega}_{MR(k-1)}, \ldots, \boldsymbol{\Omega}_{MR(k-N_7)}, Q_{H(k-1)}, \\ \quad Q_{H(k-2)}, \ldots, Q_{H(k-N_8)}] \\ \boldsymbol{Y}_H = [Q_{H(k)}] \end{cases}$$

V_z, θ, B_{1S}, A_{1C}, Q_H represent the droop rate of helicopter, the collective pitch, the longitudinal cyclic pitch, the lateral cyclic pitch and the demanded torque of the main rotor respectively.

The turbo-shaft engine dynamics model is as follows. It is mainly utilized to predict the engine state parameters. The engine dynamics can be simplified to a piece-wise-linear plant with two orders [31]. Therefore, m_1, m_2, m_3, m_4, m_5 will be set to 2.

$$\begin{aligned} \boldsymbol{Y}_E &= Pm_E(\boldsymbol{X}_E) \\ &\times \begin{cases} \boldsymbol{X}_E = [W_{f(k)}, W_{f(k-1)}, \cdots, W_{f(k-m_1)}; \\ \quad \alpha_{c(k-1)}, \alpha_{c(k-2)}, \cdots, \alpha_{c(k-m_2)}; \\ \quad Q_{E(k-1)}, Q_{E(k-2)}, \cdots, Q_{E(k-m_2)}; \\ \quad N_{g(k-1)}, N_{g(k-2)}, \cdots, N_{g(k-m_3)}; \\ N_{p(k-1)}, N_{p(k-2)}, \cdots, N_{p(k-m_4)}; \\ \quad S_{m(k-1)}, S_{m(k-2)}, \cdots, S_{m(k-m_5)}; \\ \quad T_{4(k-1)}, T_{4(k-2)}, \cdots, T_{4(k-m_5)}] \\ \boldsymbol{Y}_E = [Q_{E(k)}, N_{g(k)}, N_{p(k)}, S_{m(k)}, T_{4(k)}]^T \end{cases} \end{aligned} \tag{9}$$

where, W_f, α_c, Q_E, N_g are the fuel flow, the guide vane angle, engine output torque and the relative speed of the gas turbine separately. Based on the MRR-LSSVR predictive model, the output can be obtained after δ_u steps as:

$$\begin{aligned} \boldsymbol{Y}_E(k) &= f_E(\boldsymbol{X}_E(k)); \boldsymbol{Y}_E(k+1) \\ &= f_E(\boldsymbol{X}_E(k+1)); \ldots; \boldsymbol{Y}_E(k+\delta_p) = f_E(\boldsymbol{X}_E(k+\delta_p)) \end{aligned} \tag{10}$$

$X_E(k)$ is deduced from Eq.(9). Then let

$$\begin{cases} \bar{\boldsymbol{X}}_E = [W_f(k-2), W_f(k-1), \ldots, W_f(k+\delta_u); \\ \alpha_c(k-2), \alpha_c(k-1), \ldots, \alpha_c(k+\delta_u); \\ Q_E(k-2), Q_E(k-1), \ldots, Q_E(k+\delta_u-1); \\ N_g(k-2), N_g(k-1), \ldots, N_g(k+\delta_u-1); \\ N_p(k-2), N_p(k-1), \ldots, N_p(k+\delta_u-1); \\ S_m(k-2), S_m(k-1), \ldots, S_m(k+\delta_u-1); \\ T_4(k-2), T_4(k-1), \ldots, T_4(k+\delta_u-1)] \\ \bar{\boldsymbol{Y}}_E = [Q_E(k), Q_E(k+1), \ldots, Q_E(k+\delta_p); \\ N_g(k), N_g(k+1), \ldots, N_g(k+\delta_p); \\ N_p(k), N_p(k+1), \ldots, N_p(k+\delta_p); \\ S_{mc}(k), S_{mc}(k+1), \ldots, S_{mc}(k+\delta_p); \\ T_4(k), T_4(k+1), \ldots, T_4(k+\delta_p)]^T \\ \delta_p = \delta_u \end{cases} \tag{11}$$

Thus,

$$\bar{\boldsymbol{Y}}_E = Pm_E(\bar{\boldsymbol{X}}_E) \tag{12}$$

Similar to the helicopter demanded torque model, the flight envelope is also divided into several ones for accurate modeling. The training of a sub dynamic model is conducted in each sub envelope. The training data for MRR-LSSVR predictive model is also from exciting the component level model of turboshaft engine during autorotation.

When the predictive model obtains the predictive parameters, through the FSQP algorithm, these parameters can achieve the control target that ensures the temperature before turbine engine T_4 is not overheated and the surge margin S_m does not exceed the limited value.

$$\begin{aligned} \min J = &\sum_{i=1}^{m} \omega_1 \left(\frac{(Q_E[k+i] - Q_H[k+i])}{Q_{E,ds}} \right)^2 \\ &+ \sum_{i=1}^{m} \omega_2 \left(\frac{(N_P[k+i] - 100)}{100} \right)^2 \end{aligned} \tag{13}$$

$$s.t. \begin{cases} W_{f\min} <= W_f[k+i] <= W_{f\max} \\ \alpha_{c,\min} <= \alpha_c[k+i] <= \alpha_{c,\max} \\ \left|\Delta W_f[k+i]\right| <= \Delta W_{f\max} \\ |\Delta\alpha_c[k+i]| <= \Delta\alpha_{c,\max} \\ N_{p,\min} <= N_p[k+i] <= N_{p,\max} \\ T_4[k+i] <= T_{4,\max} \\ S_m[k+i] >= S_{m,\min} \end{cases} \quad i = 1, 2, \cdots m \tag{14}$$

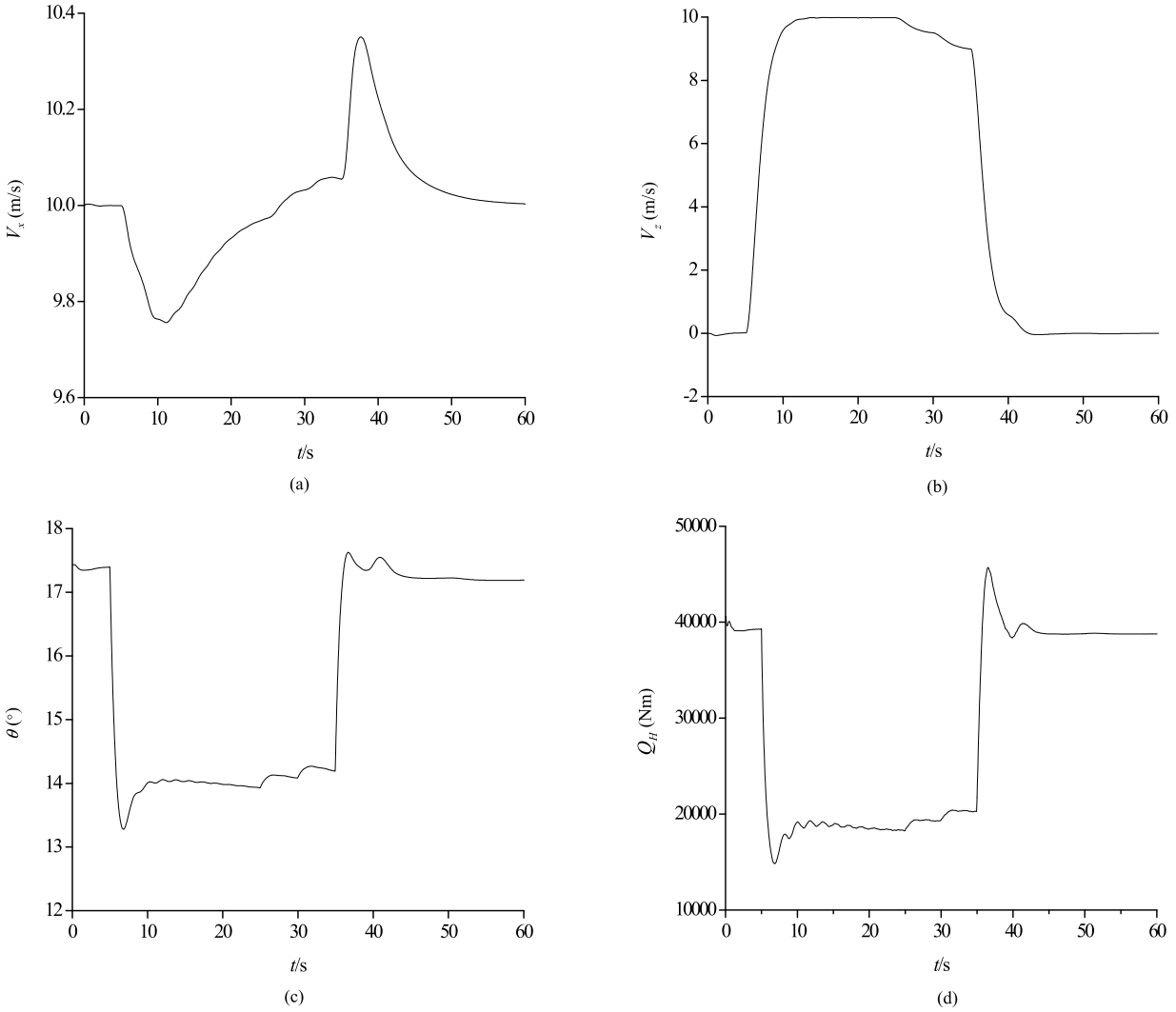

FIGURE 7. Helicopter variables in autorotation process. (a) Forward flight speed. (b) Droop rate. (c) Collective pitch. (d) Rotor demanded torque.

The control variables are the fuel flow W_f and the guide vane angle α_c. The first part of Eq. (13) decreases the difference between the torques provided by the engine and helicopter demanded torque, thereby reducing the sag of N_p, and $Q_{E,ds}$ is the set-point value of engine output torque. The second part can reduce the overshoot and sag of N_p in the optimization process, so that N_p can keep about 100%.

The simulation of helicopter autorotation process at $H = 500m$ and $V_x = 10m/s$ has been conducted. At around 4s, the helicopter enters into the autorotation, the collective pitch θ decreases rapidly (as shown in Fig. 7. (c)) to ensure that the rotor blades do not stall, and the rotor produces enough lift. At this time, the driven power is greater than the induced power, thus the rotor speed increases. When droop rate V_z decreases to the minimum, the driven power is roughly equal to the induced power. Then the rotor speed is constant, and the helicopter enters into the stable autorotation. While the helicopter is approaching the ground, through increasing θ, the V_z reduces to ensure a safe landing (as shown in Fig. 7. (b)).

At about 38s, the clutch engages, where the variations of torque and rotor speed cause the torsional vibration of the UH-60 model combined with the simplified helicopter torsional vibration model. Fig. 8. shows the engine parameters with PID and NMPC together. When executing the autorotation recovery command, the NMPC can make the W_f increase rapidly, but its growth rate will be affected by the maximal of N_p (as shown in Fig. 8. (d)). When the clutch is connected, the difference between the demanded and the output torque is large. In addition, due to inertia effect, N_p has a sharp decline in the trend. In order to make the sag of N_p small, the W_f increases at the maximum growth rate and greater torque is provided. Due to the increase in W_f, T_4 increases rapidly. At about 40s, in order to ensure that the engine does not exceed the surge boundary, the minimum limit of S_m is the constraint condition (Fig. 8. (f)). As shown in Fig. 8 (d),

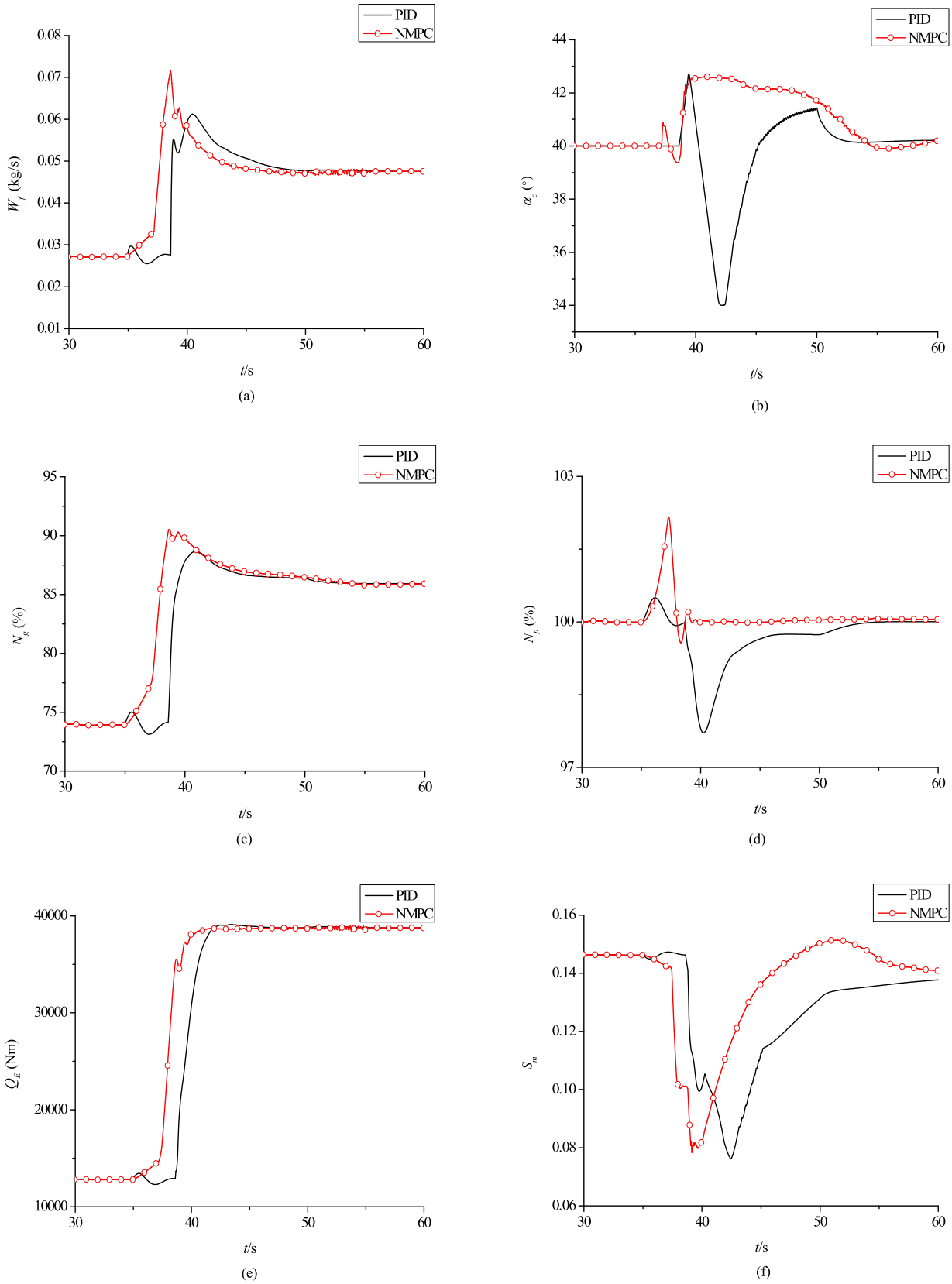

FIGURE 8. Comparison of engine parameters in autorotation recovery process. (a) Fuel flow. (b) Guide vane angle. (c) Gas turbine speed. (d) Free turbine speed. (e) Engine output torque. (f) Surge margin. (g) temperature before turbine.

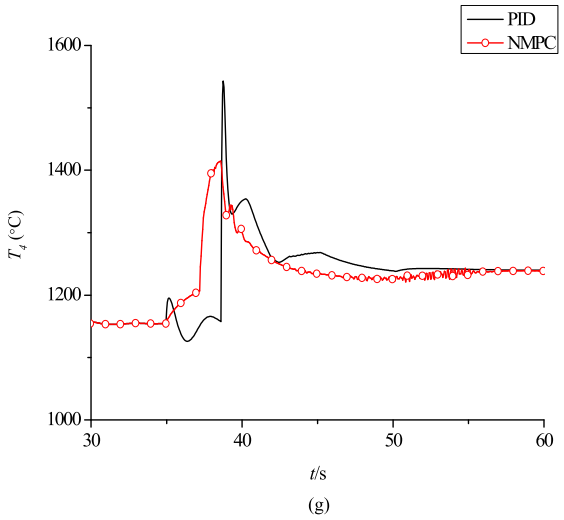

FIGURE 8. ***Continued.*** **Comparison of engine parameters in autorotation recovery process. (g) temperature before turbine.**

by reducing the difference of the demanded torque and output torque and increasing the rotor speed, the sag of N_p is reduced to less than 0.4% through the NMPC. Nevertheless, because of lack of prediction, the sag of N_p in PID control is almost 2.5%. Furthermore, during the optimization process, the NMPC can significantly decrease the stable time of N_p to 5s, which is over 20s for PID control. Compared with the conventional PID controller, the NMPC can obtain more rapid and effective dynamic response quality.

V. CONCLUSION

To damp the helicopter/engine torsional vibration and achieves fast response of the turbo-shaft engine, the adaptive notch filter and predictive controller is designed in this research. Through the variable rotor speed and autorotation recovery simulation, the following conclusions can be drawn.

(1) Through the ANF, the torsional vibration of N_p whose frequency is away from the set-point value can still be damped by 50% compared with the fixed notch filter. The FFT algorithm provides a simple and effective new control method for adaptive torsional vibration filtering, which can make up the performance and time delay once the dominant frequencies vary and has real-time and robustness.

(2) Instead of conventional PID controller, the NMPC can reduce the sag of N_p to less than 0.4%. In this case, better dynamic performance of the engine is achieved.

(3) Due to the similarity of physical mechanism, the research results can be extended to other shaft power control system researches like wind turbine, propeller, gas turbine and steam turbine.

In summary, the NMPC combined with the ANF enhances the engine's power following capacity. It filters out the variable low-frequency torsional vibration signal, and further reduces the sag and overshoot of free turbine speed. Thus, high quality control of turbo-shaft engine is realized.

APPENDIX
NOMENCLATURE

Symbol	Explanation
W_f	Fuel flow (kg/s).
α_c	Compressor guide vane angle (°).
N_g	Relative rotor speed of gas turbine (%).
N_p	Relative rotor speed of free turbine (%).
N_{pr}	Relative reference rotor speed of free turbine (%).
S_m	Engine surge margin.
T_4	Temperature before turbine (°).
$\mathbf{\Omega}_{MR}$	Main rotor speed (rad/s).
Q_H	Main rotor demanded torque (N.m).
Q_E	Turbo-shaft engine output torque (N.m).
H	Helicopter flight altitude (m).
V_z	Helicopter droop rate (m/s).
V_x	Helicopter forward flight speed (m/s).
θ	Collective pitch of the main rotor (°).
A_{1C}	Lateral cyclic pitch of the main rotor (°).
B_{1S}	Longitudinal cyclic pitch of the main rotor (°).

REFERENCES

[1] P. Haowei, *Control and Mechanism of Torsional Oscillation in New Unmanned Helicopter*. Nanjing, China: Nanjing Univ. Aeronautics Astronautics, 2009.

[2] Z. Xin, B. Zhong, and L. Haijian, "Battlefield ghost-military unmanned helicopter," *Nat. Defense Sci. Technol.*, vol. 12, pp. 31–33, 2004, doi: 10.13943/j.issn1671-4547.2004.12.007.

[3] X. Zhang, *System Design and Key Techniques Research of Fault Diagnosis and Health Management for Helicopter Transmission Train*. Changsha, China: Nat. Univ. Defense Technol., 2011.

[4] A. Pinggui, *Analysis of Lateral Vibration and Torsional Vibration of Helicopter Tail Drive System*. Nanjing, China: Nanjing Univ. Aeronautics Astronautics, 2009, doi: 10.7666/d.d076950.

[5] W. L. Joon and S. D. Mark, "Optimal sizing of composite power drive shafting," *J. Amer. Helicopter Soc.*, vol. 31, no. 1, pp. 75–83, 1986.

[6] W. Hui, C. Hua, and L. Zhi-wen, "The stability analysis of the coupled system consists of helicopter engine control system, rotor and drive train," *Helicopter Tech.*, vol. 4, no. 4, pp. 19–23, 2005, doi: 10.3969/j.issn.1673-1220.2002.04.006.

[7] Y. D. Hu, J. J. Qiu, and G. H. Qing, "Vibration analysis of the magnetism and solid of turbo-generator stator end collector ring," in *Proc. Int. Conf. Power Syst. Technol.*, 2002, pp. 2189–2192, doi: 10.1109/ICPST.2002.1047170.

[8] J.-H. Lee, Y.-H. Lee, D.-H. Kim, K.-S. Lee and I.-H. Park, "Dynamic vibration analysis of switched reluctance motor using magnetic charge force density and mechanical analysis," *IEEE Trans. Appl. Supercond.*, vol. 12, no. 1, pp. 1511–1514, Mar. 2002, doi: 10.1109/TASC.2002.1018689.

[9] R. S. Haxton and A. D. S. Barr, "The autoparametric vibration absorber," *J. Sound Vibrat.*, vol. 83, no. 3, pp. 440–443, 1971.

[10] P. Zahradnik and M. Vlcek, "Fast analytical design algorithms for FIR notch filters," *IEEE Trans. Circuits Syst. I, Reg. Papers*, vol. 51, no. 3, pp. 608–623, Mar. 2004, doi: 10.1109/TCSI.2003.822404.

[11] D. H. Lee, J. H. Lee, and J.-W. Ahn, "Mechanical vibration reduction control of two-mass permanent magnet synchronous motor using adaptive notch filter with fast Fourier transform analysis," *IET Elect. Power Appl.*, vol. 6, no. 7, pp. 455–461, 2012, doi: 10.1049/iet-epa.2011.0322.

[12] L. Jiayun and C. Hua, "The Sketch of helicopter engine digital control system," *Helicopter Techn.*, vol. 3, no. 131, pp. 43–46, 2002.

[13] R. E. Hansford and J. Vorwald, "Dynamics workshop on rotor vibratory loads prediction," *J. Amer. Helicopter Soc.*, vol. 43, no. 1, pp. 76–87, 1998.

[14] B. Smith and R. Zagranski, "Next generation control system for helicopter engines," in *Proc. 57th Annu. Forum AHS*, Washington, DC, USA, May 2001, pp. 1617–1626.

[15] B. Zhang, "Development and applications of integrated diagnostics, prognostics and health management technologies of abroad," *Comput. Meas. Control*, vol. 16, no. 5, pp. 591–594, 2008.

[16] H. Xue, J. Xiang, and X. Zhang, "Coupled helicopter rotor/propulsion/transmission system torsional vibration analytical model and coupled influence investigation," *J. Beijing Univ. Aeronaut. Astron.*, vol. 30, no. 5, pp. 438–443, 2004.
[17] M. Chen, Y. Ma, S. Liu, and J. Hong, "Rotordynamic analysis of whole aero-engine models based on finite element method," *J. Beijing Univ. Aeronaut. Astron.*, vol. 33, no. 9, pp. 1013–1016, 2007.
[18] L. S. Quan, Y. Z. Shan, and S. J. Guo, "Elimination of coupling instability using few parallel connection notch filters for helicopter rotor/power train," *J. Aerosp. Power*, vol. 21, no. 3, pp. 606–609, 2006.
[19] K. J. Åström and B. Wittenmark, *Adaptive Control*. Reading, MA, USA: Addison-Wesley, 1995, doi: http://dx.doi.org/10.2307/1269433
[20] S. Sastry and M. Bodson, *Adaptive Control: Stability, Convergence, and Robustness*. Upper Saddle River, NJ, USA: Prentice-Hall, 1989.
[21] B. J. Smith and R. D. Zagranski, "Closed loop bench testing of the next generation control system for helicopter engines," in *Proc. 58th Annu. Forum AHS*, Montreal, PQ, Canada, Jun. 2002, pp. 1041–1050.
[22] S. M. Rock and K. Neighbors, "Integrated flight/propulsion control for helicopters," *J. Amer. Helicopter Soc.*, vol. 39, no. 3, pp. 34–42, 1994.
[23] S. J. Qin and T. A. Badgwell, "A survey of industrial model predictive control technology," *Control Eng. Pract.*, vol. 11, no. 7, pp. 733–764, 2003, doi: https://doi.org/10.1016/S0967-0661(02)00186-7
[24] D. Q. Mayne, J. B. Rawlings, C. V. Rao, and P. O. M. Scokaert "Constrained model predictive control: Stability and optimality?" *Automatica*, vol. 36, no. 6, pp. 789–814, 2000, doi: https://doi.org/10.1016/S0005-1098(99)00214-9
[25] S. Garg, "Aircraft turbine engine control research at NASA Glenn Research Center," *J. Aerospace Eng.*, vol. 26, no. 2, pp. 422–438, 2013, doi: 10.1061/(ASCE)AS.1943-5525.0000296
[26] B. J. Brunell, D. E. Viassolo, and R. Prasanth, "Model adaptation and nonlinear model predictive control of an aircraft engine," in *Proc. ASME Turbo Expo Power Land, Sea, Air*, 2004, pp. 673–682, doi: 10.1115/GT2004-53780
[27] H. Richter, A. V. Singaraju, and J. S. Litt, "Multiplexed predictive control of a large commercial turbofan engine," *J. Guid. Control Dyn.*, vol. 31, no. 2, pp. 273–281, 2008, doi: https://doi.org/10.2514/1.30591
[28] J. A. Decastro, "Rate-based model predictive control of turbofan engine clearance," *J. Propuls. Power*, vol. 23, no. 4, pp. 804–813, 2007, doi: https://doi.org/10.2514/1.25846
[29] W. Jiangkang, Z. Haibo, and H. Xianghua, "Nonlinear model predictive control for the engine based on an integrated helicopter/turboshaft engine simulation platform," *Acta Aeronautica et Astronautica Sinica*, vol. 33, no. 3, pp. 402–411, 2012.
[30] J. Wang, H. Zhang, C. Yan, S. Duan, and H. Huang, "An adaptive turboshaft engine modeling method based on PS and MRR-LSSVR algorithms," *Chin. J. Aeronaut.*, vol 26, no. 1, pp. 94–103, 2013.
[31] Y. Zhao, "Support vector regressions and their applications to parameter estimation for intelligent aeroengines," Ph.D. dissertation, Dept. Aerosp. Propuls. Theory Eng., Nanjing Univ. Aeron. Astron., Nanjing, China, 2009.

YONG WANG is currently pursuing the Ph.D. degree in aerospace propulsion theory and engineering with the College of Energy and Power Engineering, Nanjing University of Aeronautics and Astronautics. His research interests include modeling, fault diagnosis, vibration cancellation, and model predictive control of aero-engines.

QIANGANG ZHENG is currently pursuing the Ph.D. degree in aerospace propulsion theory and engineering with the College of Energy and Power Engineering, Nanjing University of Aeronautics and Astronautics. His research interests include modeling, fault diagnosis, performance seeking control, and model predictive control of aero-engines.

HAIBO ZHANG received the Ph.D. degree from the Nanjing University of Aeronautics and Astronautics (NUAA) in 2005. He is currently a Professor with the College of Energy and Power Engineering, NUAA. His main research interests include modeling, fault diagnosis, vibration cancellation and optimization control of aero-engines.

LIZHEN MIAO received the master degree in aerospace propulsion theory and engineering. She is currently an Assistant Engineer with China Gas Turbine Establishment. Her research interests include modeling, fault diagnosis, vibration cancellation, and model predictive control of aero-engines.